Hindawi Publishing Corporation
Mathematical Problems in Engineering
Volume 2013, Article ID 408756, 13 pages
http://dx.doi.org/10.1155/2013/408756

Research Article

A Car-Following Model Based on Quantified Homeostatic Risk Perception

Guangquan Lu,[1] Bo Cheng,[2] Yunpeng Wang,[1] and Qingfeng Lin[1]

[1] *Beijing Key Laboratory for Cooperative Vehicle Infrastructure Systems and Safety Control, Beihang University, Beijing 100191, China*
[2] *State Key Laboratory of Automotive Safety and Energy, Tsinghua University, Beijing 100084, China*

Correspondence should be addressed to Guangquan Lu; lugq@buaa.edu.cn

Received 16 April 2013; Revised 18 September 2013; Accepted 8 October 2013

Academic Editor: Cesar Cruz-Hernandez

This study attempts to elucidate individual car-following behavior using risk homeostasis theory (RHT). On the basis of this theory and the stimulus-response concept, we develop a desired safety margin (DSM) model. Safety margin, defined as the level of perceived risk in car-following processes, is proposed and considered to be a stimulus parameter. Acceleration is assessed in accordance with the difference between the perceived safety margin (perceived level of risk) and desired safety margin (acceptable level of risk) of a driver in a car-following situation. Sixty-three cases selected from Next Generation Simulation (NGSIM) are used to calibrate the parameters of the proposed model for general car-following behavior. Other eight cases with two following cars taken from NGSIM are used to validate the model. A car-following case with stop-and-go processes is also used to demonstrate the performance of the proposed model. The simulation results are then compared with the calculations derived using the Gazis-Herman-Rothery (GHR) model. As a result, the DSM and GHR models yield similar results and the proposed model is effective for simulation of car following. By adjusting model parameters, the proposed model can simulate different driving behaviors. The proposed model gives a new way to explain car-following process by RHT.

1. Introduction

Car-following models are used to determine individual driving behaviors under continuous traffic flow, in which vehicles do not make lane changes [1]. These models are important for autonomous cruise control systems [2, 3] and are considered key evaluation tools for intelligent transportation system strategies [4–6]. A number of researchers have proposed mathematical models for car-following simulation. Brackstone and McDonald provided an excellent review on the history of car-following models proposed in the 20th century [7]. Many studies have recently explored car-following behavior to improve existing models or construct new ones [1, 8–21]. Some researchers focus on the stability analysis of car following [16, 19].

Although most of the reviewed models effectively simulate car-following behaviors and determine how car following occurs in actual scenarios, the reason why vehicles follow one another in a certain manner remains unclear. Hamdar et al. explained car-following behaviors based on the prospect theory of Kahnemann and Tversky and proposed a car following model by evaluating the gains and losses while driving [21]. Another risk-taking theory, Wilde's risk homeostasis theory (RHT) is also helpful to explain car-following behaviors [22].

Wilde defines driving behavior as a homeostatic controlled self-regulation process, in which a driver alters his/her current behavior after comparing the instantaneously experienced level of risk with the level of risk he/she is willing to take [22, 23]. According to RHT, people develop behavioral adaptation to compensate for the difference between perceived and acceptable risk [24]. This theory maintains that individuals submit to a certain level of subjectively estimated risk to their health or safety in exchange for the benefits they hope to receive from that activity [25]. Quantifying risk, especially perceived risk, is one of the key problems in RHT research. Some scholars quantify risk in RHT as "the accident

toll-the probability of an accident multiplied by its severity per unit of time, and it is assumed that this quantity is directly under the road user's control" [26]. Some researchers also use speed as a parameter for risk evaluation [26, 27]. Another method for risk investigation is self-reporting [28, 29]. Few studies quantify risk perception under unique microscopic traffic conditions, such as car following, lane changing, or merging processes.

A car-following model based on risk perception as defined in RHT and a stimulus-response model aid the understanding of car-following mechanisms and facilitate the simulation of car-following behaviors that differ depending on varied individual characteristics (the different levels of acceptable risk).

Most of the reported car-following models are based on the stimulus-response concept. The key concepts of these models revolve around defining stimulus parameters, response parameters, and response function. Using only relative speed as stimulus, Chandler et al. proposed the first linear model based on the stimulus-response concept [30, 31]. Subsequently, different stimulus parameters or response functions were used in numerous models that simulate car-following processes.

The optimized velocity approach proposed by Bando et al. assumes that car following is based on a driver's desire to maintain optimal velocity in a traffic stream [32]. The driver in the following car adjusts vehicular speed in accordance with the difference between the speed of the following vehicle and optimized velocity. Optimized velocity changes under different traffic conditions, making it an unsuitable quantitative indicator of homeostatic risk perception. Li et al. presented an empirically desired headway (EDH) model, which assumes that every car-following vehicle has an EDH at its speed and that every driver responds to stimulus from a leading vehicle [12]. Given that EDH changes with speed, it is also an unsuitable quantitative indicator of homeostatic risk perception. In the driving by visual angle model, visual angle and its changes are used as initial stimulus parameters [33]. Despite these efforts, the manner by which a driver constructs an indicator of risk perception by visual angle and its changes remains unelucidated.

The speeds of following and leading cars, along with the relative speed and spacing between them, are commonly used as an initial stimulus parameters in many models [1, 15, 32, 34]. The acceleration, velocity, relative distance, or trajectory of these cars is typically employed as response parameters [1, 15, 32–35]. However, the preset models do not precisely solve the problem of how to describe the risk perceived by drivers in car-following processes. Time-to-collision (TTC) and time headway (TH) are typically used as risk indicators in car following. Nevertheless, whether a driver uses these indicators in evaluating risk level is uncertain.

TTC is the fraction of time until collision occurs when both vehicles continue on the same course and at the same speed [36]. Some studies use it as a criterion for activating a driver support system, such as collision avoidance systems (CAS) [37]. Some researchers also consider TTC as a potential parameter for distinguishing between dangerous and safe situations [38]. Regardless of its wide application, TTC suffers from certain drawbacks in quantifying risk. A large or undefined TTC value occurs when the speed of a following car is near or equal to that of a leading vehicle. When the difference in speed between the following and leading cars is very small, the TTC is very large even at a small relative spacing between the two cars. A large TTC sometimes indicates that the difference in speed between two vehicles is small, making it an inaccurate parameter for quantifying the degree of risk in car following.

TH is the time difference between the consecutive arrival instants of two vehicles passing the measurement point on a lane. Some car-following models are based on the assumption that each driver attempts to maintain a desired following headway behind a leading vehicle [39, 40]. Although TH has been used to simulate traffic flow and adaptive cruise control, it is affected by absolute speed [41]. Because its formulation neglects the effect of relative speed, it may underestimate risk at large relative speeds.

Minimum gap and the actual gap are always used to evaluate level of risk in car following. In Gipps' model, speed of following car is determined by actual gap and desired minimum gap which are related to desired acceleration and comfortable deceleration [35]. In intelligent-driver model (IDM), interaction term of acceleration of following car is determined by actual gap and desired minimum gap which are related to comfortable braking deceleration, minimum spacing, maximum acceleration, and desired time headway [20]. We use actual gap and minimum safe gap which is related to maximum braking deceleration instead of comfortable braking deceleration to define the object level of risk as a clue to develop a quantitative indicator of subjective homeostatic risk perception in car following. In this paper, we propose a quantitative indicator of risk perception called the safety margin by measuring the speed of following and leading cars, as well as the gap between these cars. In our previous research, we found that it is a suitable quantitative indicator of homeostatic risk perception in car-following process [42]. A car-following model based on the stimulus-response concept is also proposed. In the model, the difference between perceived safety margin (perceived risk) and desired safety margin (acceptable risk) serves as the stimulus parameter. Therefore, car-following behaviors that are affected by individual characteristics (with different acceptable risks) can be simulated by adjusting the desired safety margin (DSM) and enhancing (or moderating) the sensitivity factor in the response function. Genetic algorithm (GA) is used to calibrate the parameters of the proposed model for general following behavior. The model gives a way to explain car following by RHT.

Ranjitkar et al. investigated eight models and found that the model proposed by Chandler et al. and Gazis-Herman-Rothery (GHR model) performs better than the others by producing lower percentile errors for speed and acceleration predictions [31]. Therefore, we compare the test results derived using the proposed model with those obtained by the GHR model.

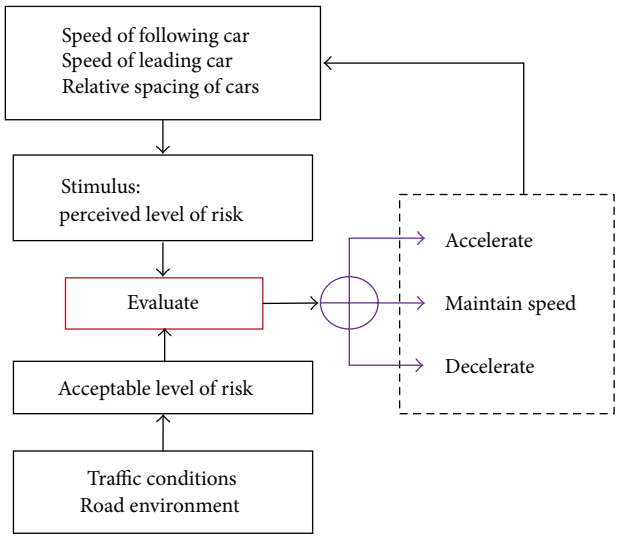

Figure 1: Car-following model based on risk perception.

2. Model Assumptions

A driver's behavior is usually influenced by car interaction, driver characteristics, and external environment [33]. Under sufficiently safe conditions, the car runs at a specific speed (desired speed) and is influenced only by the driver's characteristics and external environment. However, when a car is close to a leading car, the speed of the following car is affected by that of the leading car. The behavior of the driver in the following car depends on the speed of the leading car, distance from the leading car, and speed of the following vehicle. According to RHT, the driver of the following car adjusts the distance (or speed) in accordance with the perceived and acceptable risk levels. If the perceived level of risk is greater than the acceptable level, the driver decelerates to avoid crash.

In RHT and the stimulus-response concept, the driver of a following car responds to the stimulus (perceived level of risk) (shown in Figure 1). The driver adjusts the speed in accordance with his/her perception of risk, which is based on initial stimulus information, including the speed of the following and leading cars, relative spacing between cars, and traffic situation. However, the manner by which available information stimulates a driver and the relationship between the initial stimulus information and risk perception remain unclear. In this paper, the perception of risk is denoted by a quantified indicator of the safety margin. DSM is used to represent acceptable risk levels under different traffic environments.

In summary, a driver maintains an acceptable risk level by adjusting car speed. We assume that the driver of a following car responds to the difference between the perceived safety margin (perceived level of risk) and DSM (acceptable level of risk). In the succeeding section, we comprehensively quantify and discuss the safety margin.

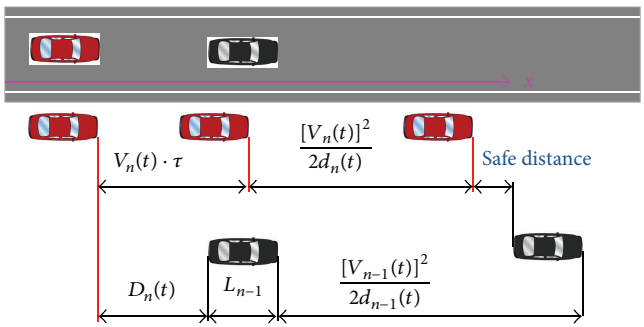

Figure 2: Braking process of a car during a car-following situation.

3. Safety Margin (Level of Risk) of Car Following

On the basis of the braking process during a car-following situation (Figure 2), we use actual gap and minimum safe gap to define level of risk as follows:

$$\xi_n(\tau,t) = \frac{V_n(t)\cdot\tau + \left([V_n(t)]^2/2d_n(t)\right)}{D_n(t)} - \frac{\left([V_{n-1}(t)]^2/2d_{n-1}(t)\right)}{D_n(t)}, \tag{1}$$

where $V_n(t)$ is the speed of the following car; $V_{n-1}(t)$ denotes the speed of the leading car; $D_n(t) = x_{n-1}(t) - x_n(t) - L_{n-1}$ is the relative spacing between the two cars, in which L_{n-1} refers to the length of the car $(n-1)$ and $x_n(t)$ and $x_{n-1}(t)$ represent the positions of the car (n) and the car itself $(n-1)$, respectively; τ represents the response time, including the driver's response time (τ_1) and brake system's response time (τ_2); $\tau = \tau_1+\tau_2$; $d_n(t)$ denotes the deceleration of the following car; and $d_{n-1}(t)$ is the deceleration of the leading car.

Risk can be described as

$$\begin{aligned}\xi_n(\tau,t) &= \frac{V_n(t)\cdot(\tau_1+\tau_2) + \left([V_n(t)]^2/2d_n(t)\right)}{D_n(t)} - \frac{\left([V_{n-1}(t)]^2/2d_{n-1}(t)\right)}{D_n(t)} \\ &= \xi_n(\tau_2,t) + \frac{V_n(t)\cdot\tau_1}{D_n(t)}.\end{aligned} \tag{2}$$

To ensure safety, actual gap cannot be less than minimum safe gap. Thus,

$$\xi_n(\tau,t) \le 1.0. \tag{3}$$

When $\xi_n(\tau,t) = 1.0$, the driver of the following car risks approaching the leading car but does not intend to collide with it in case the driver of the leading car suddenly pushes

on the brakes. The condition for keeping safe following in (3) can be denoted as

$$\frac{V_n(t)\cdot\tau_1}{D_n(t)} \le 1.0 - \xi_n(\tau_2, t). \tag{4}$$

We quantify safety margin as

$$\mathrm{SM}_n(t) = 1.0 - \xi_n(\tau_2, t). \tag{5}$$

To avoid crash, the following car must maintain a certain distance from the leading car. Thus,

$$\mathrm{SM}_n(t) \ge \frac{V_n(t)\cdot\tau_1}{D_n(t)}. \tag{6}$$

Expression (6) then becomes

$$\tau_1 \le \mathrm{SM}_n(t)\,\frac{D_n(t)}{V_n(t)}. \tag{7}$$

A large safety margin indicates that the driver of the following car has more time to respond to the movement of the leading car and that the driver has enough time to adjust relative spacing or speed.

In a car-following situation, the following car should maintain adequate space to ensure safety. When the driver of the leading car suddenly applies the brakes, the driver of the following car should follow suit to avoid a potential crash. When the emergency brake is used in the following car, its acceleration is affected by the adhesion coefficient. Adhesion coefficients are influenced by operational parameters such as speed, vertical load, and performance of road surfaces. The peak values for the adhesion coefficient are usually from 0.1 (icy road) to 0.9 (dry asphalt and concrete) [43]. The Highway Capacity Manual recommends that "vehicle acceleration rates of passenger cars accelerating after a stop range between 3 and 13 ft/s^2, while passenger car deceleration rates range between 7 and 26 ft/s^2" [44]. With reference to the test data in the literature [45, 46], the deceleration in the calculation of risk is set as

$$d_n(t) = d_{n-1}(t) = 0.75g, \tag{8}$$

where g is the acceleration due to gravity.

A driver's reaction time is difficult to determine because it is affected by many factors. While some studies determined it to be between 0.3 and 1 seconds [47], many experiments showed that a driver's reaction time ranges from 0.3 to 1.2 seconds [48]. Setti et al. investigated perception-reaction time (PRT) which corresponds to travel times to the intersection [49]. The study revealed that the observed PRTs occurred between 0.3 and 1.7 seconds, with a mean of 0.742 seconds, a median of 0.7 seconds, and a standard deviation of 0.189 seconds. A drivers' reaction time differs in the car-following process. A driver requires little reaction time when he/she adjusts speed only by acceleration pedal or brake pedal control. However, if driving requires shifting from the acceleration pedal to the brake pedal (or vice versa) to adjust speed, then a driver would need more time to react.

The response time (τ_2) of a brake system also differs under various situations because of the difference in force and speed of brake pedals. The response time of hydraulic brakes is less than that of air brakes. Bayan et al. presented detailed brake timing information obtained from the full-scale instrumented testing of a tractor semitrailer under various loads and speeds [50]. The study showed that average lag time, rise time, and steady-state delay time are 0.15, 0.33, and 0.49 seconds, respectively. After investigating the braking parameters of automobiles with and without an antilock braking system, Sokolovskij found that "the values of the time of deceleration increase of most of the Japanese and Western vehicles have not exceeded 0.2 s and remained within the limits of 0.1-0.2 s." [51]. Under emergency situations, the driver may quickly and strongly step on the brakes. Thus, we set τ_2 as 0.15 seconds.

We assume that a driver of a following car always maintains adequate spacing to prevent collision caused by emergency brake of leading car. We use minimum safe gap which is determined by maximum decelerations of following and leading cars to evaluate the risk level instead of desired minimum gap which is related to comfortable deceleration used in Gipps model and IDM [20, 35]. Consequently, the safety margin is simplified as follows:

$$\begin{aligned}\mathrm{SM}_n(t) &= 1 - \xi_n(\tau_2, t)\\ &= 1 - \frac{V_n(t)\cdot\tau_2 + \left([V_n(t)]^2/1.5g\right)}{D_n(t)}\\ &\quad - \frac{\left([V_{n-1}(t)]^2/1.5g\right)}{D_n(t)},\end{aligned} \tag{9}$$

where $\tau_2 = 0.15$ s.

Generally, drivers do not understand the response time of a brake or perceive speed or distance to an inch. They should be trained to precisely evaluate or determine safety levels (or risk levels). In our previous research, we found that safety margin almost fluctuated around a fixed value in the car-following process and was suitable to quantify homeostatic risk perception [42].

4. Car-Following Model Based on Risk Perception

As a driver follows another vehicle, he/she should adjust relative spacing (or gap) to guarantee an acceptable risk level, which can be described by the DSM. On the basis of the difference between a driver's DSM and the perceived safety margin, the driver of the following car decides to accelerate, decelerate, or maintain constant speed. The driver usually decelerates, accelerates, or maintains constant speed when the perceived safety margin is small, large, or within the domains of DSM, respectively. Given that the proposed model is based on the difference between a driver's DSM and the perceived safety margin, we call it the DSM model.

The DSM model for car following is described as follows:

$$a_{n\text{-follow}}(t+\tau) = f\left(\mathrm{SM}_n(t) - \mathrm{SM}_{nD}(t)\right) = \begin{cases} \alpha_1\left(\mathrm{SM}_n(t) - \mathrm{SM}_{nDH}(t)\right) & \mathrm{SM}_n(t) > \mathrm{SM}_{nDH}(t) \\ \alpha_2\left(\mathrm{SM}_n(t) - \mathrm{SM}_{nDL}(t)\right) & \mathrm{SM}_n(t) < \mathrm{SM}_{nDL}(t) \\ 0 & \text{else,} \end{cases} \tag{10}$$

where $a_{n\text{-follow}}(t)$ is the acceleration of a following car at time t, $\mathrm{SM}_{nDH}(t)$ is the upper limit of the DSM in a car-following condition, $\mathrm{SM}_{nDL}(t)$ denotes the lower limit of the DSM in a car-following condition, and α_1 and α_2 are the sensitivity factors for acceleration and deceleration, where $\alpha_1 > 0\ \mathrm{m/s^2}$, $\alpha_2 > 0\ \mathrm{m/s^2}$.

Despite our aim for naturalistic driving, the DSM may change because of psychological factors. In a simulation designed to analyze the primary factors that affect the car-following process, random factors are disregarded and the DSMs are considered to be fixed values that are related to driver behavior and traffic environment. Equation (10) is simplified as follows:

$$a_{n\text{-follow}}(t+\tau) = f\left(\mathrm{SM}_n(t) - \mathrm{SM}_{nD}\right) = \begin{cases} \alpha_1\left(\mathrm{SM}_n(t) - \mathrm{SM}_{nDH}\right) & \mathrm{SM}_n(t) > \mathrm{SM}_{nDH} \\ \alpha_2\left(\mathrm{SM}_n(t) - \mathrm{SM}_{nDL}\right) & \mathrm{SM}_n(t) < \mathrm{SM}_{nDL} \\ 0 & \text{else.} \end{cases} \tag{11}$$

Four constraints are imposed on (11).

(1) Maximum deceleration: the Highway Capacity Manual recommends that the deceleration of passenger car range between 7 and $26\ \mathrm{ft/s^2}$ [44]. We set a maximum deceleration restriction as $a_{n\text{-follow}}(t) \geq -8.0\ \mathrm{m/s^2}$. If $a_{n\text{-follow}}(t) < -8.0\ \mathrm{m/s^2}$, then $a_{n\text{-follow}}(t) = -8.0\ \mathrm{m/s^2}$.

(2) Maximum favorite acceleration: the Highway Capacity Manual recommends that the vehicle acceleration of passenger cars accelerating after a stop range between 3 and $13\ \mathrm{ft/s^2}$ [44]. Treiber and Kesting suggested that accelerations are within $0.8\text{–}2.5\ \mathrm{m/s^2}$ [52]. Maximum favorite acceleration of simplified Gipps' model is set to be $1.5\ \mathrm{m/s^2}$ [35, 52]. Maximum favorite acceleration of IDM is set to be $1.0\ \mathrm{m/s^2}$ [20, 52]. Typical values of a comfortable acceleration are not more than $1.5\ \mathrm{m/s^2}$ [52]. We set maximum favorite acceleration as $1.5\ \mathrm{m/s^2}$ and maximum favorite acceleration restriction as $a_{n\text{-follow}}(t) \leq 1.5\ \mathrm{m/s^2}$. If $a_{n\text{-follow}}(t) > 1.5\ \mathrm{m/s^2}$, then $a_{n\text{-follow}}(t) = 1.5\ \mathrm{m/s^2}$.

(3) Minimum speed of the following car: because of the simulated time interval, the result of calculated speed may be negative when the speed is close to zero in numerically updated process. Thus, we set the minimum speed of the following car as $V_n(t) = 0.0\ \mathrm{m/s}$, if $V_n(t) < 0.0\ \mathrm{m/s}$.

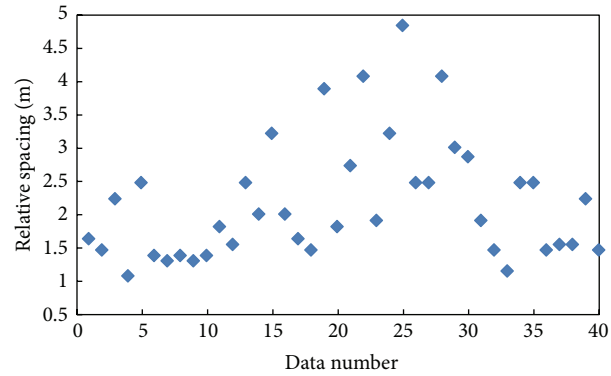

Figure 3: Relative spacing when both the following and leading car are at a stop.

(4) Minimum relative spacing: if a following car is excessively near a leading car, especially if the following car is close to stopping, the safety margin calculated using (9) will abnormally increase and cause abnormal acceleration. Thus, we set a minimum relative spacing constraint. Using 40 cases, we investigate relative spacing when both the following and leading cars are at a stop. Under this condition, the relative spacing varies from 1.07 to 4.83 m, with a mean of 2.17 m, a median of 1.90 m, and a standard deviation of 0.90 m (Figure 3). The minimum relative spacing constraint is set to be $a_{n\text{-follow}}(t+\tau) = \max\{-[V_n(t)]^2/(2 \cdot \max[(D_n(t) - g_0), 0.01]), -8.0\ \mathrm{m/s^2}\}$, if $D_n(t) < 3.0\ \mathrm{m}$, $V_n(t) > 0\ \mathrm{m/s}$, and $V_n(t) > V_{n-1}(t)$, in which g_0 is minimum favorite gap when two cars are at stop and it is set to be 1.9 m. $\max[(D_n(t) - g_0), 0.01]$ can avoid $[V_n(t)]^2/(2 \cdot \max[(D_n(t) - g_0), 0.01])$ to be unreasonable.

Treiber and Kesting summarized four criteria for acceleration or speed functions encoding the driving behavior [52]. The four criteria are as follows.

(1) The acceleration is a strictly decreasing function of the speed;

(2) the acceleration is an increasing function of the distance to the leading vehicle;

(3) the acceleration is an increasing function of the speed of the leading vehicle;

(4) a minimum gap to the leading vehicle is maintained.

Similar to the GHR model, our model also does not satisfy the second criterion strictly; that is $\partial a_{n\text{-follow}}(t)/\partial D_n(t) = \lim_{\tau \to 0}(\partial a_{n\text{-follow}}(t+\tau)/\partial D_n(t)) < 0$ for $V_n(t) < V_{n-1}(t)$.

A complete car-following model can consistently describe all situations that may arise in single-lane traffic [52]. Equation (11) can be used to describe the following situation and cannot be used to describe the free traffic situation. We add another function to describe the free traffic situation which is the same as the IDM model [52], as

$$a_{n\text{-free}}(t+\tau) = a_{\mathrm{mf}}\left[1 - \left(\frac{V_n(t)}{V_{n0}}\right)^{\delta}\right], \tag{12}$$

where $a_{n\text{-free}}(t)$ is the acceleration in free traffic at time t, a_{mf} is the maximum favorite acceleration which can be set to be 1.5 m/s^2, V_{n0} is desired speed, and δ is acceleration exponent which is set to be 4 as in the IDM model.

The proposed complete car-following model can be described as

$$a_n(t) = \min\left[a_{n\text{-follow}}(t), a_{n\text{-free}}(t)\right]. \tag{13}$$

The model can be numerically updated after setting parameters of the model, τ, SM_{nDL}, SM_{nDH}, α_1, α_2, a_{mf}, g_0, and V_{n0}. The update interval is set to be $\Delta t = \tau/j$, in which j is integer. The update scheme at step i is proposed as follows:

(1) calculate the $\text{SM}_n(i - j \cdot \Delta t)$ by (9);

(2) calculate $a_n(i)$ by $\text{SM}_n(i - j \cdot \Delta t)$ according to (11) to (13);

(3) $V_n(i) = V_n(i-1) + a_n(i-1) \cdot \Delta t$;

(4) $x_n(i) = x_n(i-1) + V_n(i-1) \cdot \Delta t + 0.5 a_n(i-1) \cdot \Delta t^2$;

(5) $D_n(i) = x_{n-1}(i) - x_n(i) - L_{n-1}$.

5. Model Calibration

As formulated in (11), five parameters should be calibrated before the model is used to simulate the car-following process. The parameters are response time τ, lower limit of the DSM SM_{nDL}, upper limit of the DSM SM_{nDH}, sensitivity factors for acceleration α_1, and sensitivity factors for deceleration α_2. We denote them as a vector,

$$\mathbf{p} = \begin{pmatrix} \tau & \text{SM}_{nDL} & \text{SM}_{nDH} & \alpha_1 & \alpha_2 \end{pmatrix}^T. \tag{14}$$

The idea of calibration is to obtain a vector $\mathbf{p}$, which can minimize the difference between measured and simulated trajectories.

5.1. Calibration Method. GA is a nonlinear optimization algorithm that simulates biological evolution, and it has been extensively used to solve complicated nonlinear optimization problems widely. It has also been used to calibrate car-following model [8]. We use GA to calibrate the parameters of the car-following model that is based on risk perception.

Speed of the following car $V_n(t)$, speed of the leading car $V_{n-1}(t)$, and relative spacing between following car and leading car $D_n(t)$ affect the car-following process. We define fitness to minimize the difference between measured and simulated speeds and the difference between measured and simulated relative spacing.

We formulate the difference between measured and simulated values of following speeds as

$$dV(t) = \frac{\left|\widehat{V}_n(t) - V_n(t)\right|}{V_n(t)}, \tag{15}$$

where $\widehat{V}_n(t)$ is the simulated speed of the following car at time t and $V_n(t)$ is the measured speed of the following car at time t.

The difference between measured and simulated values of relative spacing is formulated as

$$dD(t) = \frac{\left|\widehat{D}_n(t) - D_n(t)\right|}{D_n(t)}, \tag{16}$$

where $\widehat{D}_n(t)$ is the simulated relative spacing at time t and $D_n(t)$ is the measured relative spacing at time t.

The average differences between the measured and simulated values of following speeds and relative spacing at time t can be calculated as follows:

$$dE(t) = \frac{dV(t) + dD(t)}{2}. \tag{17}$$

All the data used to calibrate the model are discrete. Thus, we define the total average difference between measured and simulated values of following speeds and relative spacing as

$$E = \frac{1}{N}\sum_{i=1}^{N} dE(i), \tag{18}$$

where N is the number of data in a car-following process.

GA is used to find a vector $\mathbf{p}$ to minimize the E.

5.2. Calibration Result. Data from Next Generation Simulation (NGSIM) [53], a program funded by the Federal Highway Administration (FHWA), are used to calibrate the DSM model. We obtain 63 cases of car-following processes as the dataset used in calibration; these cases were collected on I-80 freeway [53]. Because different drivers have different behaviors, we calibrate $\mathbf{p}$ for each case and calculate the mean or median of parameters of all cases as the parameters of the model for general following behavior.

Figure 4 shows the box plots of the parameters calibrated using the 63 cases. The descriptive statistics of the parameters are presented in Table 1. As shown in Figure 4, the parameters vary for different cases since different drivers have different behaviors. To avoid the influence from extreme cases, we use the median of the parameters of cases for general behavior instead of the mean. That is, we set $\mathbf{p} = \begin{pmatrix} 0.50 & 0.75 & 0.94 & 6.43 & 12.22 \end{pmatrix}^T$ in the model to simulate general car-following behavior.

6. Model Validation

In this section, the DSM model is validated in real-world cases and then compared with the GHR model. It seems that the DSM and GHR models yield similar results and the proposed model is effective for simulation of car following.

6.1. GHR Model Used for Comparison. The GHR model is formulated as [7]

$$a_n(t) = c v_n^m(t) \frac{\Delta v(t-\tau)}{\Delta x^l(t-\tau)}, \tag{19}$$

where $a_n(t)$ is the acceleration of car n implemented at time t, $v_n(t)$ is the speed of the nth car, Δx and Δv refer to the

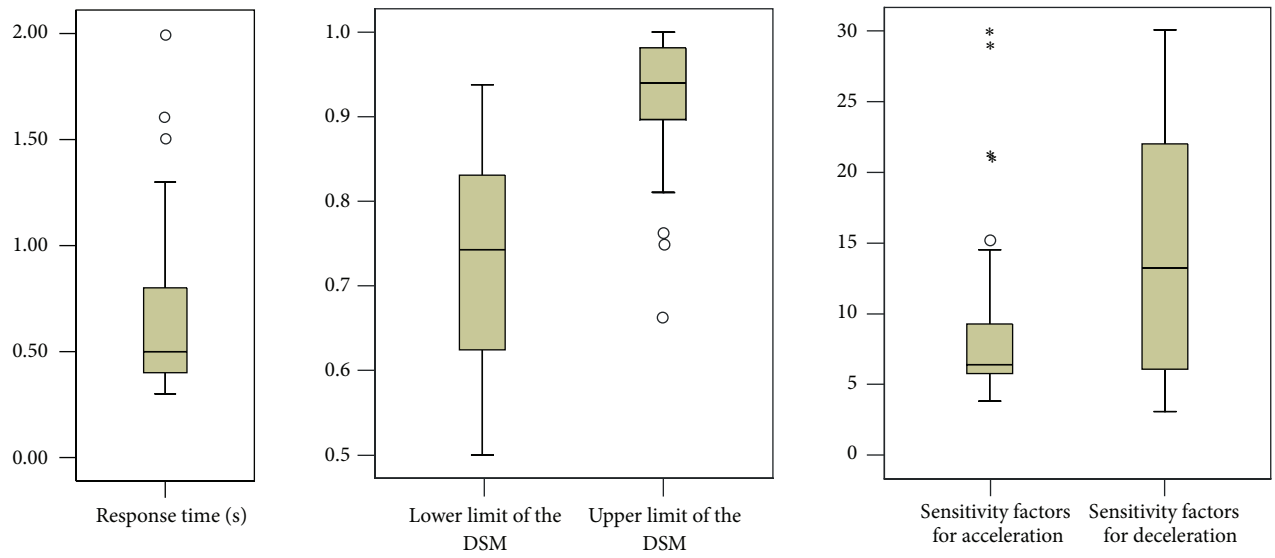

Figure 4: Box plots of parameters calibrated using 63 cases.

Table 1: Descriptive statistics of parameters calibrated using 63 cases.

	Response time τ (s)	Lower limit of the DSM SM_{nDL}	Upper limit of the DSM SM_{nDH}	Sensitivity factors for acceleration α_1 (m/s^2)	Sensitivity factors for deceleration α_2 (m/s^2)
N Valid	63	63	63	63	63
Missing	63	63	63	63	63
Mean	0.7016	0.7333	0.9297	8.4055	14.0590
Std. error of mean	0.05236	0.01673	0.00856	.66395	1.03028
Median	0.5000	0.7500	0.9398	6.4263	12.2188
Std. deviation	0.41562	0.13275	0.06796	5.26996	8.17763
Variance	0.173	0.018	0.005	27.773	66.874
Range	1.70	0.48	0.34	26.12	26.99
Minimum	0.30	0.50	0.66	3.79	3.01
Maximum	2.00	0.98	1.00	29.91	30.00

relative distance and speed, respectively, between the nth and the $(n-1)$ car (immediately subsequent car), τ is the driver reaction time, and m, l, and c represent the constants to be determined. Much work has been performed on the calibration and validation of the GHR model [7]. According to the calibrated results in the literatures, the parameters in (19) are set as $c = 1.1$, $m = 0.9$, and $l = 1$ for deceleration and $c = 1.1$, $m = -0.2$, and $l = 0.2$ for acceleration [7].

6.2. Test Results. We selected eight cases from the dataset on the vehicle trajectory of the FHWA's NGSIM project to validate the model based on quantified risk perception. The cases are the results of observations of US Highway 101 (Hollywood Freeway) in Los Angeles. The cases can be classified into four categories: speed changes a little, speed increases, speed decreases, and speed changes with increasing and decreasing. Each case includes a leading car (denoted as car 0) and two following cars (designated as car 1 and car 2). Car 1 was following car 0, and car 2 was following car 1. The measured trajectories of the leading car are used as initial data. The initial positions of the first and the second cars are set as the measured values. After response time τ, the trajectories of the first and the second cars are calculated using the DSM and GHR models.

We use the calibration result in the previous section as the parameters of the DSM model to simulate all the cases. That is, SM_{nDL}, SM_{nDH}, α_1, and α_2 are set as 0.75, 0.94, 6.43 m/s^2, and 12.22 m/s^2, respectively. Response time τ is set as 0.5 seconds for the DSM and GHR models.

The root mean square errors (RMSE) of the simulation are shown in Table 2. For all the eight cases, there are 16 pairs of car following. The average RMSE of speed of the 16 following cars for the DSM and GHR models are 1.25 and 1.38 m/s, respectively. The average RMSE of the relative spacing of the 16 following cars for the DSM and GHR models are 6.47 and 8.24 m, respectively. This seems that the proposed model in this paper is as good as the GHR model. Figure 5 shows the simulation results for one of the test cases. The figure shows that the DSM and GHR models yield similar results.

Table 2: Root mean square errors of the simulation.

Case type	Case no.	Model	Speed of car 1 (m/s)	Speed of car 2 (m/s)	Relative spacing between car 0 and car 1 (m)	Relative spacing between car 1 and car 2 (m)
Speed changes a little	1	DSM	0.84	1.62	4.87	19.34
		GHR	0.86	2.37	5.33	27.33
	2	DSM	0.99	1.15	1.96	5.66
		GHR	1.10	1.03	7.64	4.89
Speed increases	3	DSM	0.62	1.13	3.65	4.78
		GHR	0.67	1.08	3.90	4.54
	4	DSM	0.84	1.31	1.92	9.30
		GHR	0.85	1.20	1.76	11.03
Speed decreases	5	DSM	1.56	1.87	5.00	5.04
		GHR	1.78	1.98	10.32	2.94
	6	DSM	1.35	1.88	3.75	4.63
		GHR	1.93	1.90	7.89	1.72
Speed changes with increasing and decreasing	7	DSM	1.33	1.32	14.53	8.92
		GHR	1.36	1.43	14.23	9.41
	8	DSM	0.88	1.33	6.49	3.63
		GHR	1.05	1.46	14.97	3.85
Average		DSM	1.05	1.45	5.27	7.66
		GHR	1.20	1.56	8.26	8.21
		DSM	1.25		6.47	
		GHR	1.38		8.24	

6.3. Validating for Car Following with Stop-and-Go Processes. Most car-following models cannot be used to simulate stop-and-go actions in the car-following process. This function has been synthesized into the proposed model. We use a case to demonstrate it. The case is also selected from the dataset on the vehicle trajectory of the FHWA's NGSIM project and is a result of observations of US Highway 101 (Hollywood Freeway) in Los Angeles between 7:50 and 8:05 a.m. on June 15 2005 [53]. The vehicle ID of the following car is 2740 while that of the leading car is 2458. The results of the simulation in which the DSM model used are shown in Figure 6. These are compared with the findings derived using the GHR model. The parameters of the models are also set as $\mathbf{p} = (0.50 \;\; 0.75 \;\; 0.94 \;\; 6.43 \;\; 12.22)^T$.

The results of the DSM model resemble the detected data. Figure 6 shows that the DSM model can simulate stop-and-start processes. In the early stage of the car-following process (from 0 to 22.5 seconds; Figure 6), the results of both the models slightly differ from those of the case. For the GHR model, however, the acceleration (the output of the model) may be close to zero when the speed of the following car is close to zero. Consequently, the simulation may be inaccurate when the following car is close to a stop. The acceleration is zero when the speed of the following car is zero, as indicated by (19). Thus, if the following car is at a stop, it cannot start until after the leading car resumes motion in the car-following process (from 22.5 to 70 seconds; Figure 6).

7. Discussion

In spite of that the Gipps' model and the IDM contain intuitive parameters related to the driving style, such as desired accelerations, comfortable decelerations, and a desired safe time gap, they cannot to be used to describe some important aspects of the cognitive processes used by drivers, such as perception, judgment, and execution while driving [21]. Hamdar et al. assumed that a driver will have a probability density function of the acceleration he or she will adopt while given an assumed distribution of the future velocity of the leading car [21]. In our opinion, a driver adopts the acceleration or deceleration by judging that if risk level is smaller or larger than one's acceptable domain for a given state. Hamdar et al. assumed that a driver perceives risk by estimating the probability of being involved in rear-end collision. However, we aimed to propose a quantitative indicator of homeostatic risk perception. Hamdar et al. adopted prospect theory for evaluation process of gains and losses while driving, whereas a driver makes judgment by comparing perceived risk level with acceptable risk domain in DSM model.

Parameters α_1, α_2, SM_{nDL}, SM_{nDH}, and τ in the DSM model are used to describe driving behavior in the car-following process. The model can also be employed to analyze the effect of driving behavior on the car-following process by setting different parameters for different drivers.

First of all, interval $[\mathrm{SM}_{nDL}, \mathrm{SM}_{nDH}]$ is an indicator of driving behavior in adjusting speed. For instance, a small

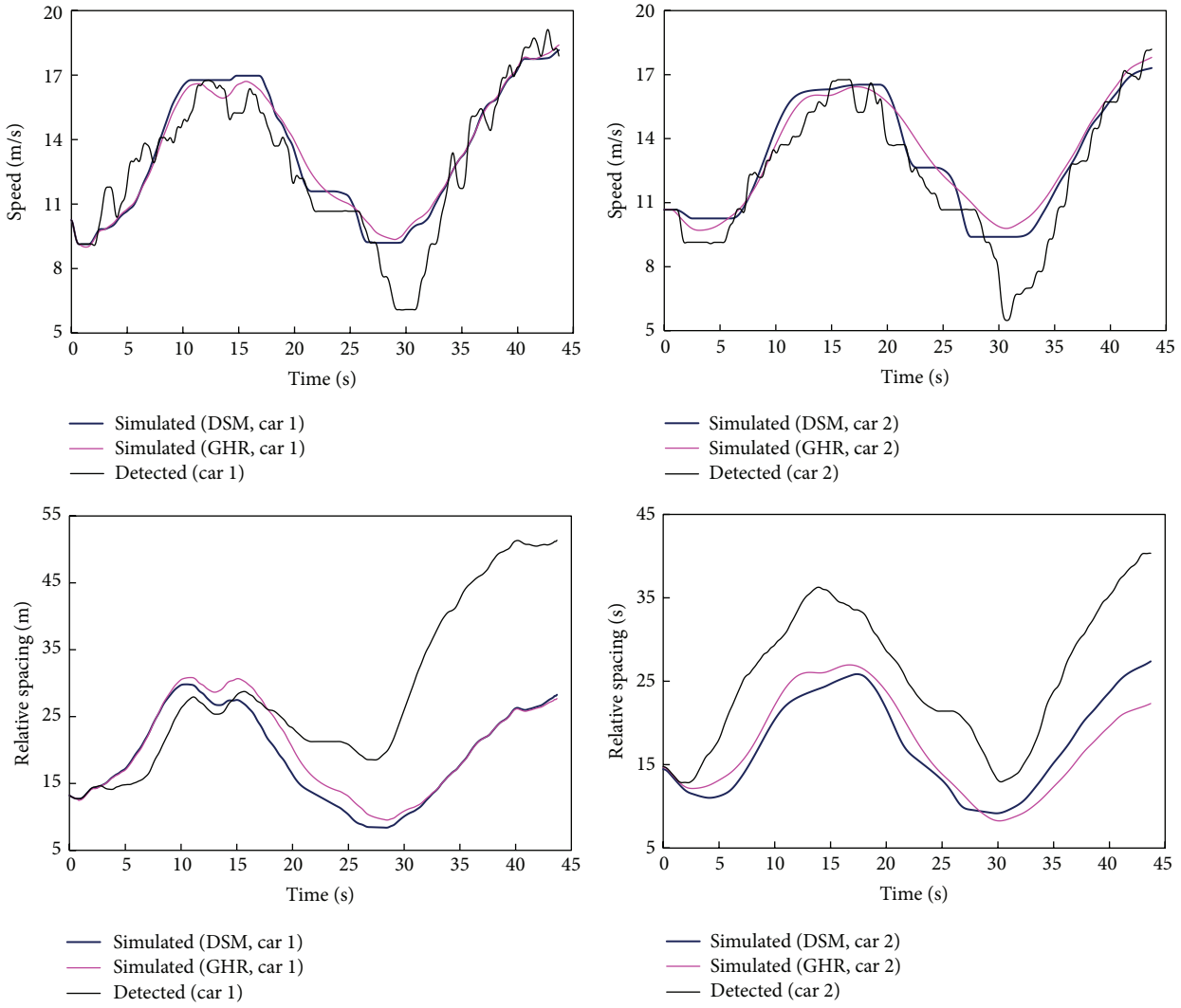

Figure 5: Simulation results on one of the test cases (case no. 7).

(SM_{nDH}-SM_{nDL}) indicates that the driver prefers frequent adjustment in speed in order to keep his/her SM within the small range. Second, α_1 and α_2 describe the preference of acceleration and deceleration. SM_{nDH}, SM_{nDL}, α_1, and α_2 are influenced by traffic circumstance, as well as by the a drivers' physiological and psychological characteristics. For example, the more careful the driver, the higher the SM_{nD} value. If a driver displays preference for sudden deceleration or acceleration, α_1 or α_2 may be increased. Finally, if a driver quickly reacts, his (her) reaction time τ may be low. The sensitivity factors, α_1 and α_2, DSM $[SM_{nDL}, SM_{nDH}]$, and reaction time τ are related to a driver's physiological and psychological characteristics. We can use the vector $\mathbf{p} = (\tau \ SM_{nDL} \ SM_{nDH} \ \alpha_1 \ \alpha_2)^T$ to describe the different behaviors of car-following for different individuals.

In the previous section, we calibrated the parameters of the model for general car-following process. The result of $\mathbf{p} = (0.50 \ 0.75 \ 0.94 \ 6.43 \ 12.22)^T$ denotes the average (or general) behavior of car-following behavior. This does not mean that good simulation results can be obtained for all car-following processes using this calibrated result because car-following behaviors are varied with driver or circumstance. For instance, careful drivers always maintain a larger relative spacing from the leading car than do aggressive drivers. By setting different DSMs, α_1, α_2, and τ values, the model can be used to describe the scenarios in which either different drivers maintain varied relative spacing under the same condition or the same driver maintains different relative spacing under various conditions.

As depicted in Figure 6, when parameters vector $\mathbf{p} = (0.50 \ 0.75 \ 0.94 \ 6.43 \ 12.22)^T$ is used to simulate the car-following process, the simulated relative spacing is greater than the measured relative spacing; the frequency of speed adjustments in simulation result is less than that measured. In this case, it seems that the driver frequently adjusts speed. A better result (shown in Figure 7) can be obtained if we adjust the $[SM_{nDL}, SM_{nDH}]$ and set parameters vector as $\mathbf{p} = (0.50 \ 0.85 \ 0.90 \ 6.43 \ 12.22)^T$ in the model. The model

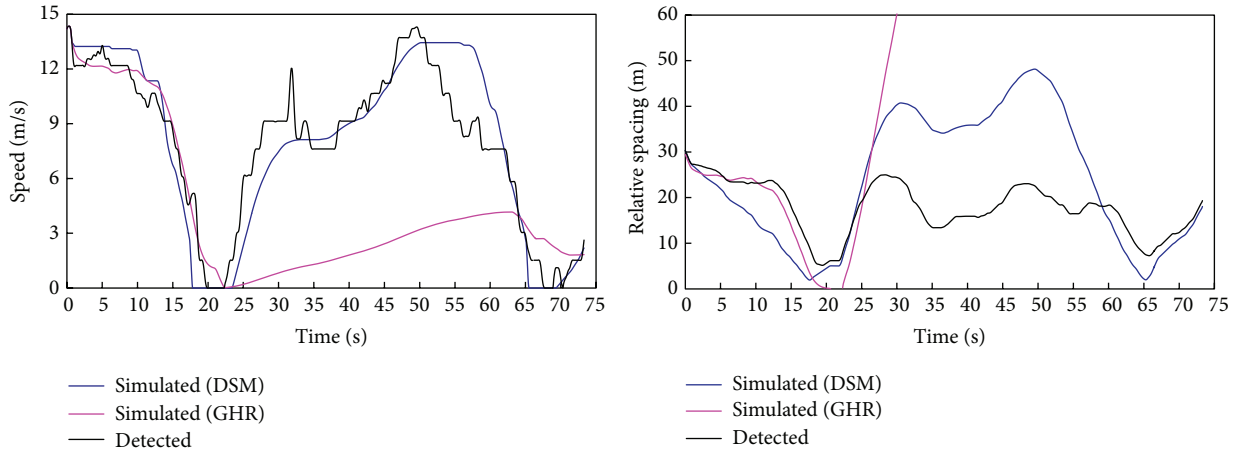

Figure 6: Simulation of the case with stop and start processes.

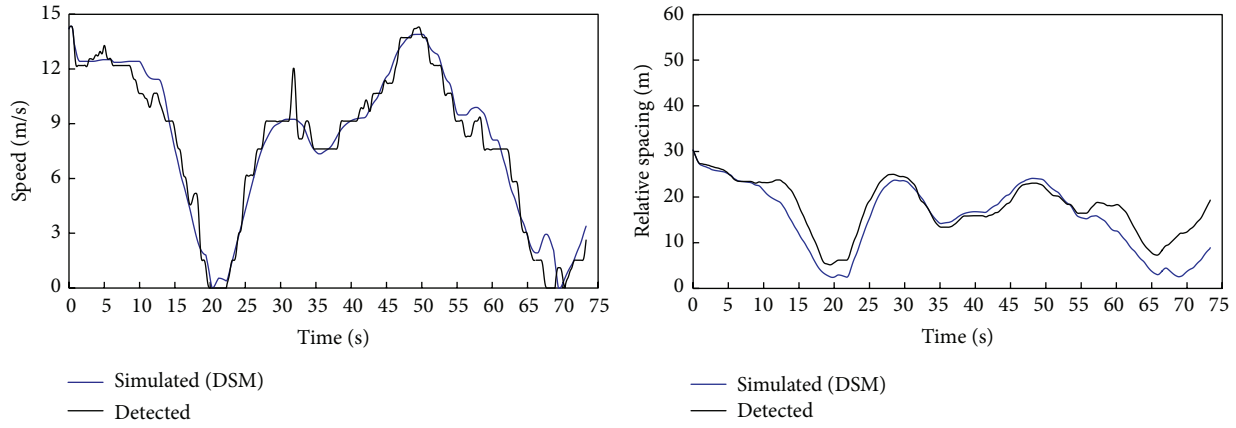

Figure 7: Simulation of the case with stop and start processes when $[SM_{nDL}, SM_{nDH}]$ is adjusted to $[0.85, 0.90]$.

facilitates the formulation of a car-following strategy that adapts to different behavior.

The proposed model can be linked with macroscopic traffic behavior. In a stationary flow, all drivers have the same target risk level of SM, denoted as SM_D. For the car-following process in stationary flow, $V_n(t) = V_{n-1}(t) = V$ and $a_n(t) = 0$. In the proposed model, average time headway can be calculated using (11) as follows:

$$H_t = \frac{\tau_2}{1 - SM_D} + \frac{\overline{L}}{V}, \tag{20}$$

where $\overline{L}$ is the average length of the cars and $\tau_2 = 0.15$ s.

Referring to Highway Capacity Manual [44], $\overline{L}$ is set to be 5.5 m, and SM_D is set to be mean of SM_{nDL} and SM_{nDH}, 0.85. The relationship between time headway and speed in the car-following process is shown in Figure 8. This relationship is similar to the result obtained by Brackstone et al. [39].

Further research should be carried out before the DSM model can be used in traffic flow analysis; issues such as distributions for reaction time τ, DSM, α_1, and α_2 should be considered. We have calibrated SM_{nDL} and SM_{nDH} which can be regarded as the thresholds for triggering deceleration or acceleration in general car-following behavior. Interval $[SM_{nDL}, SM_{nDH}]$ is the acceptable safety margin domain, but this does not mean that SM_D is uniformly distributed in the $[SM_{nDL}, SM_{nDH}]$ interval during car-following process. Further effort to identify the distribution of SM_D would

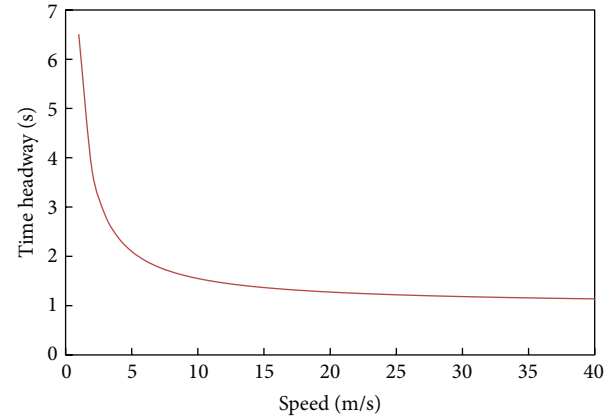

Figure 8: Relationship between time headway and speed derived using the proposed model.

be favorable for modeling the relationship between time headway and speed. Moreover, a novice driver may have larger safety margin values than a skilled driver. Investigating the distribution of DSM for different kinds of drivers in general car-following condition is important. In addition, the proposed model is appropriate for simulating the car-following process in a single lane. The application of other theories along with the DSM is also recommended for simulating the effect of other cars or traffic environments. For example, when cars in adjacent lanes may potentially move into the gap between the leading vehicle and the following vehicle, the driver of the following car may reduce the DSM to decrease (often drastically) the relative spacing ("defensive" close-following). Examining the DSM and calibrating model parameters for different drivers classified according to their characteristics in a typical traffic environment are also worthwhile research directions.

8. Conclusion

According to the stimulus-response concept, a driver decides to accelerate, decelerate, or maintain a constant speed depending on stimulus. Using RHT, we deduce that the perceived level of risk may be a suitable indicator of stimulus. Therefore, identifying one or more parameters that describe perceived risk levels during the car-following process is essential. Initial stimulus information includes the speed of the following car, speed of the leading car, relative spacing between cars, and other traffic variables. Nevertheless, how this information stimulates driver behavior remains unclear.

In this paper, the safety margin is quantified as the function of the speed of the leading car, the speed of the following car, and relative spacing during the car-following process. A new car-following model called the DSM model is proposed to determine the difference between the perceived safety margin and the DSM as the stimulus parameter. The following car accelerates (or decelerates) in response to the DSM. The proposed model serves as a potential method for investigating situations, in which different drivers maintain varied relative spacing under the same conditions, and those in which drivers maintain different relative spacing (gap) under various conditions. Different driving behaviors can be accurately described by the DSM through adjustments in the interval of the DSM and the sensitivity factors during car following. For general following behavior, 63 car-following cases are selected from datasets on I-80 freeway of NGSIM to calibrate the parameters of the proposed model. Moreover, eight cases with two following cars from datasets on US Highway 101 are used to validate the DSM model. The results are compared with those calculated by the GHR model. Both models show a slight difference. A case of car following with stop-and-go processes is used to demonstrate performance in stop-and-go following processes. These findings may provide useful insights into research on the car-following process.

Compared with existing models, the proposed model introduces a new method for explaining the mechanism underlying speed adjustment in car-following process. The characteristics of the proposed model can be summarized as follows.

(1) It is based on RHT and uses the safety margin as a quantified index of risk perception. It serves as a link between risk theory and car-following model.

(2) The parameters of the model, α_1, α_2, SM_{nDL}, SM_{nDH}, and τ, can be used to explain different car-following behaviors.

(3) By setting different DSMs, α_1, α_2, and τ values, the model can be used to describe scenarios, in which either different drivers maintain varied relative spacing under the same condition or the same driver maintains different relative spacing under various conditions.

Overall, the proposed model is a simple method for simulating different driving behaviors that are affected by the individual characteristics and car-following process can be explained by RHT using the proposed model.

Conflict of Interests

The authors declare that there is no conflict of interests regarding the publication of this paper.

Acknowledgments

This work was supported by the National High-technology R&D Program of China (2011AA110403) and the National Basic Research Program of China (2012CB725404).

References

[1] H. Gong, H. Liu, and B.-H. Wang, "An asymmetric full velocity difference car-following model," *Physica A*, vol. 387, no. 11, pp. 2595–2602, 2008.

[2] J. Mar and H.-T. Lin, "A car-following collision prevention control device based on the cascaded fuzzy inference system," *Fuzzy Sets and Systems*, vol. 150, no. 3, pp. 457–473, 2005.

[3] J. Wang, L. Zhang, D. Zhang, and K. Li, "An adaptive longitudinal driving assistance system based on driver characteristics," *IEEE Transactions on Intelligent Transportation Systems*, vol. 14, no. 1, pp. 1–12, 2013.

[4] S. Panwai and H. Dia, "Comparative evaluation of microscopic car-following behavior," *IEEE Transactions on Intelligent Transportation Systems*, vol. 6, no. 3, pp. 314–325, 2005.

[5] C. Wang and B. Coifman, "The effect of lane-change maneuvers on a simplified car-following theory," *IEEE Transactions on Intelligent Transportation Systems*, vol. 9, no. 3, pp. 523–535, 2008.

[6] L. Yu and Z. Shi, "Nonlinear analysis of an extended traffic flow model in ITS environment," *Chaos, Solitons & Fractals*, vol. 36, no. 3, pp. 550–558, 2008.

[7] M. Brackstone and M. McDonald, "Car-following: a historical review," *Transportation Research F*, vol. 2, no. 4, pp. 181–196, 1999.

[8] C. Chen, L. Li, J. Hu, and C. Geng, "Calibration of MITSIM and IDM car-following model based on NGSIM trajectory datasets,"

in *Proceedings of the IEEE International Conference on Vehicular Electronics and Safety (ICVES '10)*, pp. 48–53, QingDao, China, July 2010.

[9] H. J. Cho and Y. T. Wu, "Microscopic analysis of desired-speed car-following phenomena," in *Proceedings of the International Conference of Computational Methods in Sciences and Engineering*, Advances in Computational Methods in Sciences and Engineering, pp. 1044–1047, 2005.

[10] H. Jia, Z. Juan, and A. Ni, "Develop a car-following model using data collected by "five-wheel system"," in *Proceedings of the IEEE Intelligent Transportation Systems*, vol. 1, pp. 346–351, 2003.

[11] H. F. Jia and Z. C. Juan, "Development of a car-following model based on desired spacing," *China Journal of Highway and Transport*, vol. 13, no. 4, pp. 86–87, 2000.

[12] Z. Li, F. Liu, and Y. Liu, "A multiphase car-following model of traffic flow and numerical tests," in *Proceedings of the IEEE International Conference on Automation and Logistics (ICAL '07)*, pp. 6–10, Jinan, China, August 2007.

[13] X. Ma, "A neural-fuzzy framework for modeling car-following behavior," in *Proceedings of the IEEE International Conference on Systems, Man and Cybernetics (SMC '06)*, pp. 1178–1183, Taipei, Tiwan, October 2006.

[14] S. Maerivoet and B. de Moor, "Cellular automata models of road traffic," *Physics Reports*, vol. 419, no. 1, pp. 1–64, 2005.

[15] G. F. Newell, "A simplified car-following theory: a lower order model," *Transportation Research B*, vol. 36, no. 3, pp. 195–205, 2002.

[16] P. Ranjitkar, T. Nakatsuji, Y. Azuta, and G. S. Gurusinghe, "Stability analysis based on instantaneous driving behavior using car-following data," *Transportation Research Record*, no. 1852, pp. 140–151, 2003.

[17] S. Panwai and H. Dia, "Neural agent car-following models," *IEEE Transactions on Intelligent Transportation Systems*, vol. 8, no. 1, pp. 60–70, 2007.

[18] A. Schadschneider, "Cellular automata models of highway traffic," *Physica A*, vol. 372, no. 1, pp. 142–150, 2006.

[19] M. Tanaka, P. Ranjitkar, and T. Nakatsuji, "Asymptotic stability and vehicle safety in dynamic car-following platoon," *Transportation Research Record*, no. 2088, pp. 198–207, 2008.

[20] M. Treiber, A. Hennecke, and D. Helbing, "Congested traffic states in empirical observations and microscopic simulations," *Physical Review E*, vol. 62, no. 2, pp. 1805–1824, 2000.

[21] S. H. Hamdar, M. Treiber, H. S. Mahmassani, and A. Kesting, "Modeling driver behavior as sequential risk-taking task," *Transportation Research Record*, vol. 2088, no. 1, pp. 208–217, 2008.

[22] G. J. S. Wilde, "The theory of risk homeostasis: implications for safety and health," *Risk Analysis*, vol. 2, no. 4, pp. 209–225, 1982.

[23] F. M. Streff and E. S. Geller, "An experimental test of risk compensation: between-subject versus within-subject analyses," *Accident Analysis & Prevention*, vol. 20, no. 4, pp. 277–287, 1988.

[24] R. M. Trimpop, "Risk homeostasis theory: problems of the past and promises for the future," *Safety Science*, vol. 22, no. 1–3, pp. 119–130, 1996.

[25] K. Malnaca, "Risk homeostasis theory in traffic safety," in *Proceedings of the 21th ICTCT Workshop*, Riga, Latvia, 2008.

[26] W. H. Janssen and E. Tenkink, "Considerations on speed selection and risk homeostasis in driving," *Accident Analysis & Prevention*, vol. 20, no. 2, pp. 137–142, 1988.

[27] T. Assum, T. Bjørnskau, S. Fosser, and F. Sagberg, "Risk compensation—the case of road lighting," *Accident Analysis & Prevention*, vol. 31, no. 5, pp. 545–553, 1999.

[28] J. A. Thomas and D. Walton, "Measuring perceived risk: self-reported and actual hand positions of SUV and car drivers," *Transportation Research F*, vol. 10, no. 3, pp. 201–207, 2007.

[29] B. A. Morrongiello, J. Lasenby, and B. Walpole, "Risk compensation in children: why do children show it in reaction to wearing safety gear?" *Journal of Applied Developmental Psychology*, vol. 28, no. 1, pp. 56–63, 2007.

[30] R. E. Chandler, R. Herman, and E. W. Montroll, "Traffic dynamics: studies in car following," *Operations Research*, vol. 6, no. 2, pp. 165–184, 1958.

[31] P. Ranjitkar, T. Nakatsuji, and A. Kawamura, "Car-following models: an experiment based benchmarking," *Journal of the Eastern Asia Society for Transportation Studies*, vol. 6, pp. 1582–1596, 2005.

[32] M. Bando, K. Hasebe, A. Nakayama, A. Shibata, and Y. Sugiyama, "Dynamical model of traffic congestion and numerical simulation," *Physical Review E*, vol. 51, no. 2, pp. 1035–1042, 1995.

[33] G. J. Andersen and C. W. Sauer, "Optical information for car following: the Driving by Visual Angle (DVA) model," *Human Factors*, vol. 49, no. 5, pp. 878–896, 2007.

[34] D. C. Gazis, R. Herman, and R. W. Rothery, "Nonlinear follow the leader models of traffic flow," *Operations Research*, vol. 9, no. 4, pp. 545–567, 1961.

[35] P. G. Gipps, "A behavioural car-following model for computer simulation," *Transportation Research B*, vol. 15, no. 2, pp. 105–111, 1981.

[36] K. Vogel, "A comparison of headway and time to collision as safety indicators," *Accident Analysis & Prevention*, vol. 35, no. 3, pp. 427–433, 2003.

[37] R. V. Horst and J. Hogema, "Time-to-collision and collision avoidance systems," in *Proceedings of the 6th ICTCT Workshop*, Austrian Road Safety Board, Salzburg, Austria, 1993.

[38] R. Miller and Q. Huang, "An adaptive peer-to-peer collision warning system," in *Proceedings of the 55th Vehicular Technology Conference (VTC Spring '02)*, vol. 1, pp. 317–321, May 2002.

[39] M. Brackstone, B. Waterson, and M. McDonald, "Determinants of following headway in congested traffic," *Transportation Research F*, vol. 12, no. 2, pp. 131–142, 2009.

[40] T. Chen, B. Jia, X.-G. Li, R. Jiang, and Z.-Y. Gao, "Synchronized flow in a cellular automaton model with time headway dependent randomization," *Chinese Physics Letters*, vol. 25, no. 8, pp. 2795–2798, 2008.

[41] M. Fiorani, M. Mariani, L. Minin, and R. Montanari, "Monitoring time-headway in car-following task," in *Proceedings of the 28th Annual CHI Conference on Human Factors in Computing Systems (CHI EA '08)*, pp. 2143–2146, Florence, Italy, April 2008.

[42] G. Lu, B. Cheng, Q. Lin, and Y. Wang, "Quantitative indicator of homeostatic risk perception in car following," *Safety Science*, vol. 50, no. 9, pp. 1898–1905, 2012.

[43] C. Ünsal and P. Kachroo, "Sliding mode measurement feedback control for antilock braking systems," *IEEE Transactions on Control Systems Technology*, vol. 7, no. 2, pp. 271–281, 1999.

[44] TRB, *Highway Capacity Manual*, Transportation Research Board, Washington, DC, USA, 2000.

[45] J. G. Wallingford, B. Greenlees, and S. Christoffersen, "Tire-roadway friction coefficients on concrete and asphalt surfaces applicable for accident reconstruction," SAE Technical Paper 900103, 1990.

[46] D. Vangi and A. Virga, "Evaluation of emergency braking deceleration for accident reconstruction," *Vehicle System Dynamics*, vol. 45, no. 10, pp. 895–910, 2007.

[47] Y.-H. Wu, H. Yuan, H. Chen, and J. Li, "A study on reaction time distribution of group drivers at car-following," in *Proceedings of the 2nd International Conference on Intelligent Computing Technology and Automation (ICICTA '09)*, pp. 452–455, Changsha, China, October 2009.

[48] R. Ge, W. Zhang, and Z. Wang, "Research on the driver reaction time of safety distance model on highway based on fuzzy mathematics," in *Proceedings of the International Conference on Optoelectronics and Image Processing (ICOIP '10)*, pp. 293–296, Haikou, China, November 2010.

[49] J. R. Setti, H. Rakha, and I. El-Shawarby, "Analysis of brake perception-reaction times on high-speed signalized intersection approaches," in *Proceedings of the IEEE Intelligent Transportation Systems Conference (ITSC '06)*, pp. 689–694, Toronto, Canada, September 2006.

[50] F. P. Bayan, A. D. Cornetto III, A. Dunn, and E. Sauer, "Brake timing measurements for a tractor-semitrailer under emergency braking," *SAE International Journal of Commercial Vehicles*, vol. 2, no. 2, pp. 245–255, 2010.

[51] E. Sokolovskij, "Experimental investigation of the braking process of automobiles," *Transport*, vol. 20, no. 3, pp. 91–95, 2005.

[52] M. Treiber and A. Kesting, *Traffic Flow Dynamics: Data, Models and Simulation*, Springer, 2013.

[53] NGSIM, "Home of the Next Generation SIMulation Community," 2011, http://ngsim-community.org.